Diyala Agricultural Sciences Journal, 2026, Vol. (18) No. 1: 52-67 ISSN: 2073-9524
eISSN: 2310-8746

Projected Impacts of Climate Change on Wheat (*Triticum aestivum*) Yield and Water Productivity Using AquaCrop Model

Hassan mutahhar amer[1*], Abdullah mohammed yaya[1], Adel mohammed al-weshali[1]

[123]Department of Agricultural Engineering and Modern Technologies, College of Agriculture, Food, and Environment, Sana'a University, Yemen.

*Corresponding author: hassan.amer@su.edu.ye

Article history:
Received: 6 November 2025
Accepted: 28 February 2026
Published: 30 June 2026

Keywords:
AquaCrop model, Deficit Irrigation, Weather, Wheat Yield, Water productivity.

Abstract

The AquaCrop model developed by FAO, practical tool for simulating yield responsein improving water management and increasing productivity. This study evaluates the future impact of climate change on local wheat yield and water productivity, using the AquaCrop model. Field trials were conducted over two growing seasons (2023, 2024) under three irrigation treatments: full irrigation (I_1), moderate deficit irrigation (I_2) (75% of full irrigation), and severe deficit irrigation (I_3) (50% of full irrigation). The AquaCrop model was calibrated with data from the 2023 season and validated using data from the 2024 season, using three global climate models (CNRM-CM5, GFDL-ESM2M, and EC-Earth) under two emission scenarios (RCP4.5, RCP8.5), considering both constant and elevated atmospheric CO_2 concentrations. The results showed in both seasons that treatment (I_1) produced the highest grain yield (1.73,1.60 ton ha^{-1}) respectively, while moderate deficit treatment(I_2) achieved the greatest water productivity (WP_{ET}) (0.51, 0.52 kg m^{-3}) respectively, The AquaCrop model accurately simulated grain yield and biomass across irrigation treatments Determination coefficient (R^2) indicated strong complete between measured and predicted values for grain yield and biomass (100, 100, and 88, 85%) respectively, the Climate Is expected to experience rising temperatures and variable rainfall in both Maximum and Minimum Temperatures in the (RCP4.5 and RCP8.5) scenarios. Results showed a reduction in wheat yields when atmospheric CO_2 concentrations were assumed constant. In contrast, elevated CO_2 conditions increased simulated grain yield and reduced actual evapotranspiration. The study shows the importance of the AquaCrop model as a decision-support tool for irrigation planning, management, and climate adaptation in water-scarce regions.

https://dx.doi.org/10.52951/dasj.26180104

This article is open-access under the CC BY 4.0 license (http://creativecommons.org/licenses/by/4.0/).

Introduction

Yemen's agriculture is predominantly rain-fed poses a significant challenge to agricultural production, particularly in regions with limited water such as Sana'a City. Rising temperatures, altered rainfall patterns, and more frequent droughts will exacerbate water scarcity, leading to reduced crop yields. Research has shown that Yemen is highly vulnerable to climate change, with future climatic conditions expected to negatively impact cereal production, especially wheat, the country's staple food (Al-Dobaee, 2016).

Wheat production in Yemen is constrained by declining cultivated areas, low productivity, and increasing pressure on groundwater resources. The total wheat-cultivated area in Yemen is estimated at approximately 587,323 ha, with a production of about 861,409 ton and an average yield of 1.5 ton ha^{-1} in Sana'a City, wheat cultivation covers nearly 284 ha, producing approximately 409 tons with an average yield of 1.44 ton ha^{-1} (Ministry of Agriculture and Irrigation, 2024). Under these conditions, improving irrigation efficiency and optimizing water use have become essential strategies to sustain wheat production and enhance food security.

Deficit irrigation has been widely recognized as an effective approach for increasing water productivity by reducing irrigation inputs while minimizing yield losses. However, the success of deficit irrigation strategies depends on crop response to water stress and local climatic conditions. Therefore, reliable crop simulation models are increasingly used to support irrigation planning and climate adaptation strategies. Among these models, The AquaCrop model developed by the Food and Agriculture Organization (FAO) (Steduto *et al.,* 2012), practical tool for simulating yield responsein improving water management and increasing productivity under water stress climate variability which has proven effective (Halawa, 2022; Al-Saadi, 2022), and the AquaCrop model has been successfully applied in various agro-climatic worldwide to simulate crop grain yield and water use under different irrigation systems and climate change scenarios. Previous studies have demonstrated its effectiveness in Ethiopia (Tirfi and Oyekale, 2022), Iran (Aghajanloo and Nikbakht, 2023), Turkey (Kale and Madenoğlu, 2018), Greece (Dercas *et al.,* 2022), Egypt (Nematallah and Kasem, 2021), Syria (Al-Durai *et al*., 2025), and Iraq (Hassan *et al.,* 2023), and in Yemen under local conditions (Saif *et al.,* 2020).

Meanwhile, Bouras *et al.,* (2019), in Morocco, found that rising temperatures lead to 30% a decrease in productivity. Asseng *et al.* (2015) found 6% a decrease in global wheat yield for each additional degree of temperature. Whereas Ainsworth and Long (2005) explained the effect of carbon dioxide on plant physiology. This study aims to provide scientific guidance for sustainable irrigation management and climate change adaptation strategies for wheat production in water-scarce.by: Assess the effects of different irrigation treatments (full irrigation, deficit irrigation) on wheat yield and water productivity, projecting future (2020-2059) changes in yield and water productivity using an ensemble of climate models and scenarios, analyzing the interacting effects of CO_2, temperature, and rainfall.

Materials and Methods

Study Site

Experiments were conducted at the farm of the College of Agriculture, Foods, and Environment, Sana'a University (15.364°N, 44.182°E; 2264 m elevation) over the 2023 and 2024 growing seasons.

Daily climatic data, were obtained from the nearby meteorological station operated by the General Authority of Meteorology and Civil Aviation at Sana'a Airport. These data were used as climatic inputs for the AquaCrop model (version 7.1).

Experimental design and Crop management

The experiment was arranged in a randomized complete block design (RCBD) with three irrigation treatments and three replications. The irrigation treatments consisted of:

I_1: Full irrigation (100% of crop evapotranspiration actual, Etc)

I_2: Deficit irrigation (75% of Etc)

I_3: Deficit irrigation (50% of Etc)

Each experimental plot had an area of 12 m² (4 m × 3 m). Surface basin irrigation was used, and a spacing of 2 m was maintained between plots and replications to minimize lateral water movement.

Local wheat (Triticum aestivum) was sown on 10 July 2023 and 10 July 2024 for the first and second seasons, respectively, and harvested on 7 October 2023 and 5 October 2024. Nitrogen fertilizer (46% N) was applied at a total rate of (250 kg ha^{-1}), split into two equal applications: the first at sowing and the second 45 days after planting. Weed and pest control practices were applied uniformly across all treatments to avoid non-water stress effects.

AquaCrop Model Calibration and Validation

The AquaCrop model was calibrated using 2023 data from the first treatment (I_1) (no stress). The main parameters calibrated included vegetative growth, root depth, phenological stages, and stress coefficients Table 1. The calibration process was repeated several times (Raes *et al.,* 2023) to ensure complete agreement between measured and model-simulated values.

Following the calibration process, the model was evaluated and validated. Data from the 2024 growing season were used to assess the performance of the AquaCrop model in predicting wheat yield at the experimental site, without modifying the previously calibrated model.

Considerations taken into account when preparing data files in the AquaCrop model

1. Wind speed was converted from a height of 10 m to 2 m, as the climate data for Sana'a were obtained from the airport station

2. A climate file was prepared for the study area with daily data for the two seasons (2023-2024).

3. Projects were also created for the model, and other files were prepared for each project, starting with the crop file. Wheat crop files were selected and stored in the program database.

4. It was modified using the daily calendar (CD) system according to the aforementioned crop data and then converted to a cumulative temperature calendar (GDD).

5. Irrigation files were created, and the irrigation date and amount of irrigation water added to each irrigation were determined. They were calibrated. A field file was then created, including the fertilization level and weed control with default values of "Moderate" for calibration. The option "preventing surface runoff" was set, considering that agriculture must be in closed basins. A soil file was created based on the aforementioned data. An initial moisture file was prepared and calibrated. A project file was created for each case and run to obtain the variable values after the calibration process.

Table 1. Standards used to calibrate local wheat in the AquaCrop model

Index	Value
Initial vegetation cover (CCO). vegetation growth coefficient (%)	3.38
Maximum vegetation cover (CCX). Maximum vegetation cover (%)	95
Specific soil water depletion factor for leaf growth, upper limit	0.1
Specific soil water depletion factor for leaf growth, lower limit	0.45
Specific water stress factor for leaf growth, shape factor	4.5
Soil water depletion factor for porous control	0.8
Soil water stress factor for porous control, shape factor	2.5
Soil water depletion factor associated with vegetative arrest	0.7
Soil water depletion factor associated with vegetative arrest, shape factor	2.5
Seedling emergence from planting date (days)	6
Time to reach maximum vegetative coverage (ccx) from planting date (days)	55
Time to reach maximum rooting depth (days)	50
Maximum rooting depth (Zx) m	0.6
Start of senescence from planting date (days)	65
Reaching the stage maturity from planting date (days)	90
Time to flowering (days)	50
Harvest index (HIO) (days)	39
Flowering duration (days)	12
Planting date	10/07/2023
Harvest date	7/10/2023

Experimental Measurements and Calculations

Soil moisture measurements

To estimate the gravimetric soil moisture, soil samples were taken at specific time intervals, including the final and initial soil water content during the calculation period (at the first time after irrigation and at the second time before the next irrigation).

Soil Sampling and Analysis

Before agriculture, soil samples were collected from two depth intervals (0–30 cm and 30–60 cm) for physical, chemical, and textural analyses. Soil texture was determined using the hydrometer method, while bulk density, field capacity, permanent wilting point, porosity, and saturated hydraulic conductivity were determined using standard laboratory procedures.

Chemical analyses included soil pH, electrical conductivity (EC), organic matter content, total nitrogen, available phosphorus, and exchangeable potassium. Irrigation water quality was also analyzed for EC and pH to assess its suitability for irrigation. The soil at the experimental site was classified as sandy clay loam in the upper layer and clay loam in the lower layer. As shown in Tables (2, 3, 4), Physical, chemical, and mechanical analyses of soil, analysis results of the added water sample, the electrical conductivity value (EC=0.4 ds m^{-1}) and the pH=8, which is good water for irrigation.

Table 2. Mechanical analysis of soil

Depth (cm)	Sand (%)	Silt (%)	Clay (%)	Texture Classification
0-30	50	24	26	Sandy Clay Loam
30-60	33	30	37	Clay Loam

Table 3. Physical analysis of soil

Depth (cm)	Pb (g cm^{-3})	ρS (g cm^{-3})	FC (%)	PWP (%)	Sat (%)	n (%)	TAW (mm)	Ksat (mm hr^{-1})
0-30	1.46	2.608	20.08	10.98	30.27	44.02	132.86	8.72
30-60	1.38	2.579	25.81	13.10	33.82	46.50	175.49	3.31

Where ρb, ρS=bulk and actual density, FC=Field capacity=wilting point permanent, Sat=saturation, n=porosity, TAW=Available water, and Ksat=hydraulic connection.

Table 4. Chemical analysis of soil

Depth (cm)	PH	EC (ds m^{-1})	CaCo3 (%)	O.M (%)	N (%)	C (%)	C/N	K (ppm)	P (ppm)
0-30	8.22	0.63	8.79	0.92	0.08	0.53	0.53	236.57	14.71
30-60	8.35	0.36	7.10	1.01	0.13	0.59	0.59	196.27	13.62

Irrigation scheduling and Water efficiency

Irrigation scheduling was performed using the FAO CropWat 8.0 model based on local climatic data and crop growth stages. Irrigation was applied at 10-day intervals throughout the growing season. as shown in (Table 5). The total amount of irrigation water applied varied according to the irrigation treatment. Water productivity indices were calculated following FAO methodology Water efficiency was calculated using Equations 1 and 2, according to the methodology of Steduto *et al.* (2012) as follows:

$$WP_{ET} = \frac{Y}{ETc} \ldots\ldots\ldots..(1)$$

$$WP_{I} = \frac{Y}{I} \ldots\ldots\ldots\ldots..(2)$$

Where: WP_{ET} is the yield per cubic meter (the net water consumption) (irrigation and rainfall, ET_C) or water use efficiency (kg m^{-3}), WP_I is the yield per cubic meter of irrigation water (kg m^{-3}), *Y* represents the actual grain yield of the crop (ton ha^{-1}), Etc. is the net water consumption of the crop (m^3 ha^{-1}), and I is the total irrigation volume (m^3 ha^{-1}).

The crop response coefficient to water stress was calculated using Stewart's equation (3) which quantifies the relative decrease in production resulting from a decrease in water consumption.

$$Ky = \frac{(1 - \frac{Y}{Y_{max}})}{(1 - \frac{ETc}{ET_{max}})} \ldots\ldots\ldots\ldots\ldots.(3)$$

Where: *Y* actual wheat crop production under deficit irrigation (ton ha^{-1}). Y_{max} indicates maximum production under full irrigation in the absence of water stress (ton ha^{-1}). Eta represents water consumption under deficit irrigation (m^3 ha^{-1}). ET_{max} represents water consumption under full irrigation (m^3 ha^{-1}).

Table 5. Shows the amount of irrigation water applied for different irrigation treatments

Irrigation No.	Month	Irrigation date	Irrigation rate in (mm) Irrigation treatments		
			I_1	I_2	I_3
1	July	10/7/2023	17	13	9
2	July	20/7/2023	17	13	9
3	July	30/7/2023	28	21	14
4	August	9/8/2023	36	29	18
5	August	19/8/2023	46	37	23
6	August	29/8/2023	64	47	32
7	September	8/9/2023	67	50	33
8	September	18/9/2023	69	51	34
9	September	28/9/2023	38	29	19
Total during one season			382	292	191

Climate data

Daily climate data obtained for the two growing seasons (2023, 2024) include (Tmax, Tmin) temperatures, relative humidity, wind speed, precipitation rainfall, and sunshine duration.

This data was obtained from the General Authority of Meteorology and Civil Aviation at Sana'a Airport. This is the climate data required for the AquaCrop modeling process, and Figure 1 shows the average climate data under the two growing seasons.

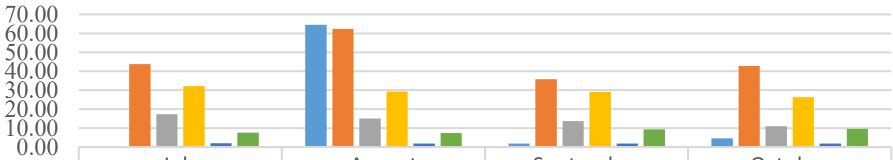

	July	August	September	October
Rainfall (mm)	0.50	64.45	1.75	4.50
Relative humidity (%)	43.67	62.37	35.77	42.60
Min temperature (°C)	17.18	15.10	13.74	10.99
Max temperature (°C)	32.14	29.34	29.12	26.21
Wind m/s	1.99	1.91	1.88	1.76
Sunshine hr/day	7.61	7.39	9.37	9.59

Figure 1. Shows climatic data for the study area in the growing seasons (2023, 2024)

Projections, Scenarios, and the Climate Models

Future climate scenarios were generated using three climate models: CNRM-CM5, GFDL-ESM2M, and EC-Earth, under two representative concentration pathways (RCP4.5 and RCP8.5). Simulations were conducted for two future periods: near future (2020–2039) and mid-century future (2040–2059), using the historical period (1986–2005) as a reference. Simulations were run under two atmospheric CO_2 conditions: constant (350 ppm) and elevated (as per RCP trajectories).

Climate data were obtained from bias-corrected regional climate datasets developed under the RICCAR/CORDEX framework. Two atmospheric CO_2 concentration conditions were considered: constant CO_2 (350 ppm) and increased CO_2 corresponding to each RCP scenario. Average outputs from the three climate models were used as inputs for AquaCrop simulations (ESCWA, 2017; ESCWA, 2019).

Statistical analysis

Data analysis was grain yield and biomass performed using Statistix 8.1 for grain yield and biomass. Mean comparisons were performed using the least significant difference test at the 0.05 probability level. Model accuracy was evaluated using the coefficient of determination (R^2), Mean Bias Error (MBE), Mean Absolute Error (MAE), Root Mean Square Error (RMSE), and the Willmott index of agreement (d).

Following established evaluation criteria, as indicated by (Akol *et al.,* 2024; Willmott *et al.,* 2013), according to the following equations:

$$R^2 = 1 - \frac{\sum_{i=1}^{n} (Oi - Si)^2}{\sum_{i=1}^{n} (Oi - Oavg\mathrm{I})^2} \ldots\ldots\ldots (4)$$

Oi = field values, *Si* = simulated values, *n* = number of values used in the comparison, and *Oavg* = average of the observed values.

$$\mathrm{MBE} = \frac{\sum_{\mathrm{i}=1}^{\mathrm{n}} (\mathrm{Si} - \mathrm{Oi})}{\mathrm{n}} \ldots\ldots\ldots\ldots\ldots (5)$$

$$\mathrm{MAE} = \frac{\sum_{\mathrm{i}=1}^{\mathrm{n}} |(\mathrm{Oi} - \mathrm{Si})|}{\mathrm{n}}$$

$$\mathrm{RMSE} = \sqrt{\frac{\sum(\mathrm{Si} - \mathrm{Oi})^2}{\mathrm{n}}} \ldots\ldots (6)$$

$$\mathrm{d} = 1 - \frac{\sum_{\mathrm{i}=1}^{\mathrm{n}} (\mathrm{Oi} - \mathrm{Si})^2}{\sum_{\mathrm{i}=1}^{\mathrm{n}} [(|\mathrm{Si} - \mathrm{Oi}| + |\mathrm{Oi} - \mathrm{Oavg}|)^2]} \ldots\ldots\ldots (7)$$

Results and Discussion

Yield, and Water consumption

Yield, above-ground biomass, and water consumption of local wheat differed significantly among irrigation treatments during both growing seasons (2023,2024), as Tables (6, 7). Full irrigation (I_1) resulted in the highest seasonal water consumption, averaging 392.37 mm in 2023 and 366.21 mm in 2024. Correspondingly, this treatment produced the highest grain yield, with mean values of (1.73- and 1.60- ton ha^{-1}) in the seasons respectively, as well as the highest biomass production (5.27- and 5.05- ton ha^{-1}).

Moderate deficit irrigation (I_2) reduced seasonal water consumption to 292.93 mm in 2023 and 268.59 mm in 2024. This reduction in applied water resulted in lower grain yield compared with full irrigation, with yields of 1.49-and 1.38-ton/ha for the two seasons, respectively. biomass production under (I_2) followed a similar trend, with values of (4.51- and 4.39- ton ha^{-1}).

Severe deficit irrigation (I_3) recorded the lowest water consumption (196.17 mm in 2023 and 180.77 mm in 2024) and the lowest grain yield and biomass in both seasons. Grain yield under (I_3) averaged (0.68- and 0.65- ton ha^{-1}), while biomass production was (2.10- and 2.00-ton ha^{-1}) in 2023 and 2024, respectively. Differences in grain yield and biomass between irrigation treatments in both seasons were statistically significant at $p \leq 0.05$.

The findings of this study confirm that irrigation level is a key determinant of wheat grain yield and water productivity under the agro-conditions of Sana'a city. Full irrigation consistently resulted in the highest grain yield and biomass, as it effectively minimized water stress throughout the growing season, particularly during critical phenological stages such as flowering and grain filling.

Adequate soil moisture during these stages sustains photosynthetic activity, supports efficient assimilate translocation, and promotes optimal grain development.

Conversely, yield reductions observed under deficit irrigation treatments reflect the cumulative physiological effects of water stress on crop growth. Limited water availability constrains leaf expansion, accelerates senescence, and reduces canopy cover, thereby lowering radiation interception and biomass accumulation. These processes ultimately result in fewer grains per spike and reduced yield. Similar responses have been widely reported for crop grown under water-limited conditions (Al-Saadi, 2022; Al-Durai *et al.,* 2025; Hassan *et al.,* 2023).

Water efficiency and Crop response to water stress

Tables (6, 7) show that the different irrigation treatments led to different results for both water productivity based on evapotranspiration (WP_{ET}) and irrigation water productivity (WP_I) measurements. The highest (WP_{ET}) values for both growing seasons resulted from moderate deficit irrigation (I_2), which produced (0.51and 0.52 kg m^{-3}) results in 2023 and 2024, respectively. The (WP_I) values between 0.51 and 0.48 kg m^{-3}.

The water productivity results showed their lowest values under severe deficit irrigation (I_3), which produced (WP_{ET}) measurements between (0.35 and 0.36 kg m^{-3}) and (WP_I) measurements between (0.36 and 0.34 kg m^{-3}) throughout both growing seasons. The water productivity results for full irrigation (I_1) showed intermediate values, which produced the highest grain yield.

The crop response coefficient to water stress (Ky) was lowest under moderate deficit irrigation (0.55 in 2023 and 0.51 in 2024), indicating that yield reductions were proportionally smaller than reductions in water application under this treatment.

The moderate deficit irrigation treatment (I_2) produced the highest water productivity, although its grain yield was lower than full irrigation treatment(I_1).

The data show that controlled deficit irrigation improves water-use efficiency because the yield reduction was less than the water reduction. Deficit irrigation emerges as an effective water conservation method for arid and semi-arid regions because wheat plants can endure moderate water stress without experiencing major yield losses.

The deficit irrigation treatments showed lower water productivity (WP_{ET}) and irrigation efficiency (WP_I) results compared to the full irrigation treatment (I_1) results obtained during both growing seasons.

The treatment values recorded for (I_1), (I_2), and (I_3) during the second season (2024) showed a decline when compared to the first season (2023) because climatic changes created conditions which decreased grain productivity.

These results are in line with previous studies findings (Tirfi and Oyekale, 2022; Aghajanloo and Nikbakht, 2023; Kale and Madenoğlu, 2018; Dercas *et al.,* 2022).

Table 6. Shows values of grain yield, biomass, (WP_{ET}), and (WP_I) for the local wheat in the 2023 season

Irrigation treatment	Water consumption (ET_C)	Total irrigation (I)	yield measured	Biomass measured	WP_{ET}	Wp_I	Ky
	(mm)	(mm)	(ton ha^{-1})	(ton ha^{-1})	(kg m^{-3})	(kg m^{-3})	
I_1	392.37	382	1.73 $_a^*$	5.27 $_a^*$	0.44	0.45	
I_2	292.93	290	1.49 $_b^*$	4.51 $_b^*$	0.51	0.51	0.55
I_3	196.17	191	0.68 $_c^*$	2.10 $_c^*$	0.35	0.36	1.21
LS D 0.05			0.066	0.012			
CV			2.23	0.13			

*Different letters indicate a significant difference at 0.05 difference between treatments, with mean comparisons using the least significant difference (LSD) test.

Table 7. Shows values of grain yield, biomass, (WP_{ET}), and (WP_I) for the local wheat in the 2024 season

Irrigation treatment	Water consumption (ET_C)	Total irrigation (I)	yield measured	Biomass measured	WP_{ET}	Wp_I	Ky
	(mm)	(mm)	(ton ha^{-1})	(ton ha^{-1})	(kg m^{-3})	(kg m^{-3})	
I_1	366.21	382	1.60 $_a^*$	5.05 $_a^*$	0.44	0.42	
I_2	268.59	290	1.38 $_b^*$	4.39 $_b^*$	0.52	0.48	0.51
I_3	180.77	191	0.65 $_c^*$	2.00 $_c^*$	0.36	0.34	1.17
LS D 0.05			0.048	0.070			
CV			1.98	0.92			

*Different letters indicate a significant difference at 0.05 difference between treatments, with mean comparisons using the least significant difference (LSD) test.

Model Calibration and Validation and Compatibility quality analysis

Calibration data (2023 Season)

To assess the performance of the AquaCrop model, simulated outputs were compared with field-measured data for grain yield and biomass using observations from the first agricultural season of 2023, as presented in Table 8. Following model calibration, AquaCrop model demonstrated high accuracy in simulating both grain yield and biomass, with coefficients of determination (R^2) approaching (100%) for both variables. Mean bias error (MBE) and mean absolute error (MAE) values were minimal, ranging from (0.01 to -0.01 and 0.02 to 0.05), respectively.

Table 8. Shows the grain yield and biomass values measured, and values simulated by the AquaCrop model, Compatibility analysis in the 2023 season

Irrigation treatment	Yield measured (ton ha^{-1})	Yield simulation (ton ha^{-1})	Biomass measured (ton ha^{-1})	Biomass simulation (ton ha^{-1})
I_1	1.73	1.71	5.27	5.09
I_2	1.49	1.47	4.51	4.43
I_3	0.68	0.66	2.10	2.86
Compatibility quality analysis				
R^2	1.00		1.00	
MBE	0.01		-0.01	
MAE	0.02		0.05	
RMSE	0.02		0.06	
d	1.00		1.00	

The root mean square error (RMSE) was approximately (2%) for grain yield and (6%) for biomass. In addition, a strong agreement between observed and simulated values was confirmed by the Willmott index (d), which reached (100%) for both variables, indicating excellent model reliability. These results are in line with previous research findings (Nematallh and Kasem, 2021; Halawa, 2022).

Validation data (2024 Season)

Model validation using data from the second agricultural season of 2024.Table 9 indicated that AquaCrop model maintained a high level of accuracy in simulating grain yield and biomass.

The coefficient of determination (R^2) ranged from (0.88 to 0.85%) for both variables. Low values of MBE and MAE were recorded, ranging from (−0.04 to−0.16and from 0.05 to 0.16), respectively. The RMSE values were approximately (10%) for grain yield and (35%) for biomass.

A high level of agreement between measured and simulated values was also observed, as reflected by Willmott's index (d), which reached (93%) for grain yield and (92%) for biomass. Despite this strong performance, relative declines in R^2 values and increases in MBE, MAE, and RMSE were observed in the 2024 season compared with 2023, and a slight decline in model performance during the validation season highlights its sensitivity to interannual climatic variability and changing soil conditions.

Variations in temperature and rainfall between seasons can influence crop phenology and stress responses.to the reduction in grain yield and biomass during 2024 relative to their higher values in 2023. This observation is consistent with previous studies (Nematallh and Kasem, 2021; Halawa, 2022).

Table 9. Shows the grain yield and biomass values measured, and values simulated by the AquaCrop model, Compatibility analysis in the 2024 season

Irrigation treatment	Yield measured (ton ha^{-1})	Yield simulation (ton ha^{-1})	Biomass measured (ton ha^{-1})	Biomass simulation (ton ha^{-1})
I_1	1.60	1.58	5.05	5.09
I_2	1.38	1.38	4.39	4.43
I_3	0.65	0.90	2.00	2.86
Compatibility quality analysis				
R^2	0.88		0.85	
MBE	-0.04		-0.16	
MAE	0.05		0.16	
RMSE	0.10		0.35	
d	0.93		0.92	

Expected climate change in the study area

Climate expected from climate models (CNRM-CM5, GFDL-ESM2M, and EC-Earth) indicated a consistent increase in both (Tmax) and (Tmin) temperatures in the RCP4.5 and RCP8.5 scenarios as Tables (10, 11). The largest increase in max temperature (2.47°C) was projected for the period (2040–2059) under RCP8.5 using the EC-Earth model.

Table 10. Shows expected changes in max and min temperatures and Rainfall under RCP 4.5 and the models (CNRM-CM5, GFDL-ESM2M, EC-Earth) for Sana'a*

Climatic factors	The model	Average rate for historical years	Expected changes	
			Near future	Medium future
		1986-2005	2020-2039	2040-2059
Rainfall (mm)	CNRM-CM5	148.38	16.91	-12.97
Max Temperatures (°C)		23.95	0.97	1.67
Min Temperatures (°C)		12.68	0.53	0.76
Rainfall (mm)	GFDL-ESM2M	135.1	-15.56	-5.95
Max Temperatures (°C)		24.02	1.17	1.65
Min Temperatures (°C)		12.68	0.63	0.91
Rainfall (mm)	EC-Earth	148.46	-9.68	-10.1
Max Temperatures (°C)		24	1.01	1.82
Min Temperatures (°C)		12.69	0.5	0.85

*Note: Expected changes for the near (2020-2039) and middle (2040-2059) periods compared to the historical period (1986-2005).

Expected changes in rainfall varied among models and scenarios. In general, a decline in mean annual rainfall was projected for the mid-century period (2040–2059), particularly under the RCP8.5 scenario. The greatest reduction in rainfall (16.18 mm) was expected by the GFDL-ESM2M model for the same period.

Table 11. Shows expected changes in max and min temperatures and Rainfall under RCP 8.5 and the models (CNRM-CM5, GFDL-ESM2M, EC-Earth) for Sana'a*

Climatic factors	The model	Average rate for historical years	Expected changes	
			Near future	Medium future
		1986-2005	2020-2039	2040-2059
Rainfall (mm)	CNRM-CM5	151.28	19.79	- 11.04
Max Temperatures (°C)		23.98	1.17	2.10
Min Temperatures (°C)		12.67	0.59	1.01
Rainfall (mm)	GFDL-ESM2M	122.54	- 6.94	- 16.18
Max Temperatures (°C)		24.07	1.30	2.36
Min Temperatures (°C)		12.70	0.66	1.22
Rainfall (mm)	EC-Earth	145.65	1.12	- 1.79
Max Temperatures (°C)		24.0	1.39	2.47
Min Temperatures (°C)		12.69	0.65	1.34

*Note: Expected changes for the near (2020-2039) and middle (2040-2059) periods compared to the historical period (1986-2005).

Projected Impact of climate change on yield

Simulations indicated that expected changes in grain yield were strongly influenced by both irrigation regime and atmospheric CO_2 concentration Table 12, and Figure 2. Under increased CO_2 concentrations, grain yield was projected to increase across all irrigation treatments under both RCP scenarios. The highest expected yield (2.82 ton ha^{-1}) was obtained under full irrigation (I_1), relative Change (63.06%) during the 2040–2059 period under RCP8.5. compared to the base period (1.73 ton ha^{-1}) (2023, 2024).

In contrast, simulations assuming constant CO_2 concentrations generally resulted in reduced grain yield relative to the baseline period, particularly under deficit irrigation treatments (I_2, I_3). Deficit irrigation (I_3) consistently produced the lowest projected yields across (0.59 ton ha^{-1}) relative change (-13.23.06%) during the 2020–2039 period under RCP4.5 compared to the base period (0.68 ton ha^{-1}).

Climate change expected indicate that rising temperatures and altered rainfall patterns will substantially influence future wheat yield in the study area. Under scenarios with elevated atmospheric CO_2 concentrations, grain yield increases in both near- and medium-term future periods. This response reflects the partial compensation of temperature- and water-related stresses by CO_2 effects, which enhance photosynthetic rates and improve water-use efficiency.

The positive impact of elevated CO_2 is primarily associated with physiological mechanisms such as increased carbon assimilation and partial stomatal closure. Reduced stomatal conductance lowers transpiration losses Ainsworth and Long (2005), conserving and mitigating water stress, particularly under irrigated conditions. As a result, crop productivity can be maintained.

However, the magnitude of the CO_2 effect observed in this study is smaller than that reported in some global assessments. For example, (Asseng *et al.* 2015; Bouras *et al.,* 2019). Expected wheat yield declines driven largely by temperature increases. This apparent discrepancy can be explained by differences in spatial scale, irrigation management, and modeling assumptions.

While global studies often emphasize rainfed systems and average climatic conditions, the present study incorporates irrigation and explicitly simulates CO_2 effects, which can partially offset thermal stress at the local scale. These findings highlight climate change impacts on crop productivity. When CO_2 is assumed remain constant, yield reductions are consistently expected under future climate scenarios.

This underscores the dominant negative influence of rising temperatures and rainfall variability on wheat productivity in the absence of CO_2. Therefore, expected yield increases under future climates should be interpreted as conditional outcomes that depend strongly on CO_2 trajectories and effective water management. ‹(ESCWA, 2019; Saif *et al.,* 2020).

Table 12. Shows the grain yield under RCP4.5 and RCP8.5, for irrigation treatments and Expected periods compared to the base period for Sana'a

Irrigation treatment	Baseline period	Expected changes							
		Near future		future medium		Near future		future medium	
	2023-2024	2020-2039		2040-2059		2020-2039		2040-2059	
	Climate scenario	RCP4.5				RCP8.5			
	State CO_2	F	Inc	F	Inc	F	Inc	F	Inc
	The average grain yield (Y) (ton ha^{-1})								
I_1	1.73	1.55	1.8	1.91	2.36	2	2.36	1.59	2.82
	Rel (%)*	-10.69	3.76	10.23	36.59	15.72	36.18	-8.15	63.06
	Abs (ton ha^{-1})*	-0.19	0.06	0.18	0.63	0.27	0.63	-0.14	1.09
I_2	1.45	1.04	1.21	1.41	1.75	1.73	2.04	1.04	1.33
	Rel (%)	-28.03	-16.26	-2.42	21.11	19.72	41.18	-28.03	-7.96
	Abs (ton ha^{-1})	-0.41	-0.24	-0.04	0.31	0.29	0.6	-0.41	-0.12
I_3	0.68	0.59	0.69	0.82	1.01	1.1	1.27	0.62	0.79
	Rel (%)	-13.24	1.47	20.59	48.53	61.76	86.76	-8.82	16.18
	Abs (ton ha^{-1})	-0.09	0.01	0.14	0.33	0.42	0.59	-0.06	0.11

* Rel= Relative Change, Abs= Absolute Change, F=fixed CO_2, and In=Increase CO_2

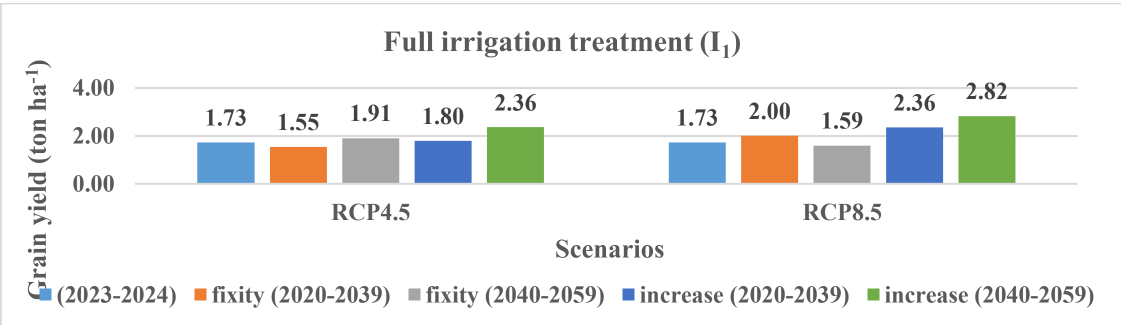

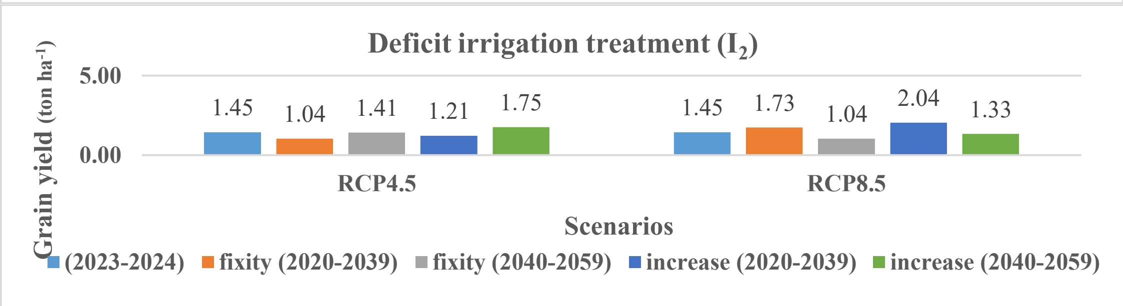

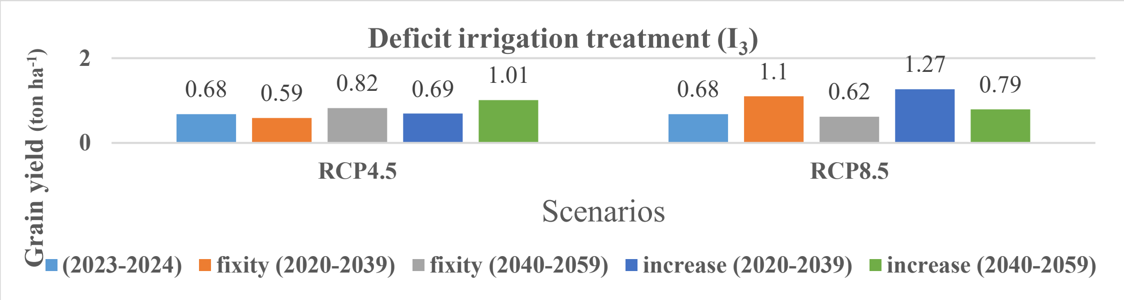

Figure 2. illustrates the grain yield under RCP4.5 and RCP8.5, during the expected periods, compared to the baseline period for irrigation treatments, fixed and increased CO_2 for Sana'a

Projected Impact of Climate Change on Evapotranspiration

The expected changes in evapotranspiration actual (ETc) varied depending on the irrigation treatment, climatic scenario, and carbon dioxide concentration Table 13, and Figure 3. Under constant carbon dioxide concentration, (ETc) was generally lower than in the reference period, particularly under full irrigation (I_1). The lowest expected (ETc) (341.0mm) was observed under the RCP8.5 scenario, with a relative change of (-13.09%) during the period (2040–2059), compared to the baseline period (392.37mm) (2023, 2024).

This reflects the reduced transpiration resulting from partial stomatal closure. This response is well supported by plant physiological theory and experimental evidence and has led to improved water use efficiency, in particular. In contrast, simulations that also assumed a constant CO_2 concentration showed an overall increase in actual evapotranspiration compared to the baseline period, particularly under the deficit irrigation treatments (I_2, I_3). Extreme deficit irrigation (I_3) achieved the highest predicted evapotranspiration (293.60 mm), with a relative change of (49.67%) over the period (2020–2039) under the RCP8.5 scenario, compared to the base period (196.17 mm).

Table 13. Shows the evapotranspiration actual under RCP4.5 and RCP8.5, for irrigation treatments and Expected periods compared to the base period for Sana'a

Irrigation treatment	Baseline period	Expected changes							
		Near future		future medium		Near future		future medium	
	2023-2024	2020-2039		2040-2059		2020-2039		2040-2059	
	Climate scenario	RCP4.5				RCP8.5			
	State CO_2	F*	Inc	F	Inc	F	Inc	F	Inc*
	The evapotranspiration actual (ETc) (mm)								
I_1	392.37	351.00	349.50	363.00	358.30	366.30	363.60	341.00	351.70
	Rel (%)*	-10.54	-10.93	-7.49	-8.68	-6.64	-7.33	-13.09	-10.37
	Abs(mm) *	-41.37	-42.87	-29.37	-34.07	-26.07	-28.77	-51.37	-40.67
I_2	292.93	312.80	311.80	323.70	320.90	344.30	342.10	306.20	304.10
	Rel (%)	6.78	6.44	10.50	9.55	17.54	16.79	4.53	3.81
	Abs(mm)	19.87	18.87	30.77	27.97	51.37	49.17	13.27	11.17
I_3	196.17	270.30	269.70	270.20	269.30	293.60	292.50	262.80	260.70
	Rel (%)	37.79	37.48	37.74	37.28	49.67	49.11	33.97	32.89
	Abs(mm)	74.13	73.53	74.03	73.13	97.43	96.33	66.63	64.53

* Rel= Relative Change, Abs= Absolute Change, F=fixed CO_2, and In=Increase CO_2.

This increase can be attributed to the increased sensitivity of crops to water stress. These results indicate that the dynamics of actual evapotranspiration are influenced by the interaction between irrigation systems and atmospheric CO_2 concentrations, and not solely by climatic factors. This reflects the increased sensitivity and responsiveness of crops to water stress under these treatments; findings harmonize with studies by Hassan *et al.* (2023); Halawa (2022).

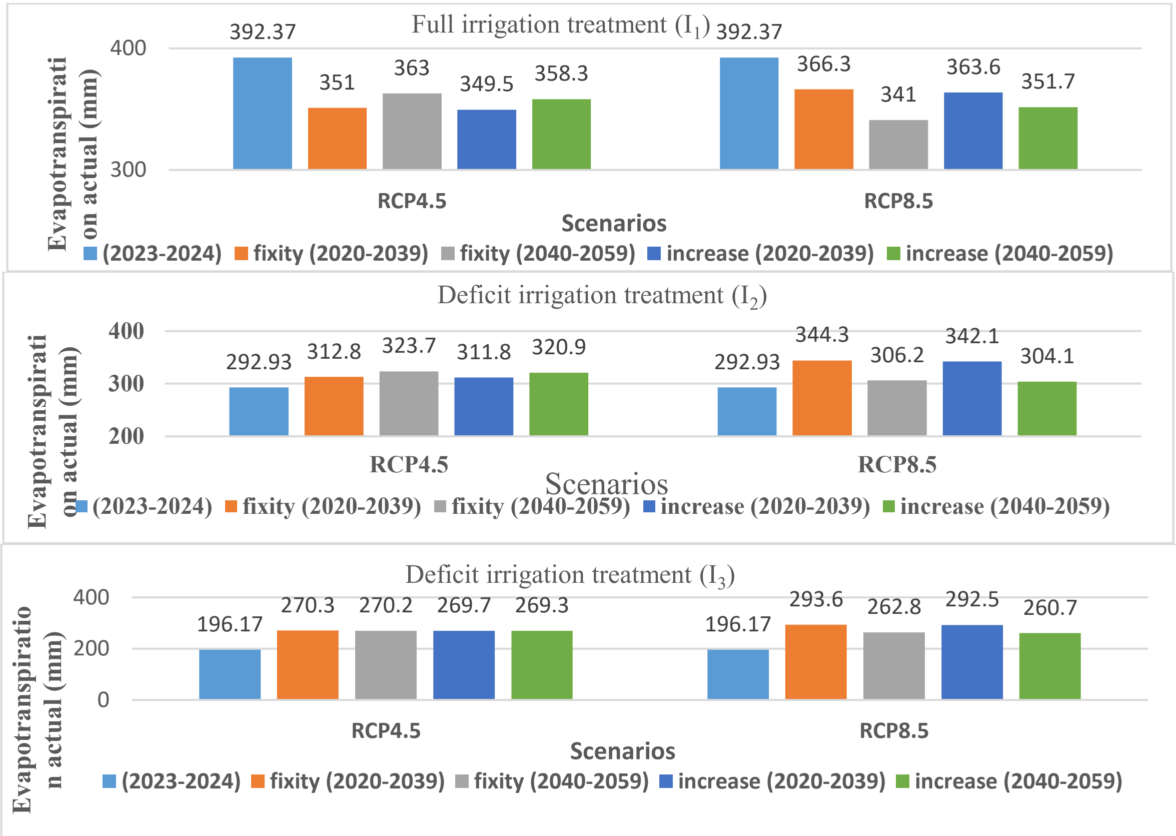

Figure 3. illustrates the evapotranspiration actual under RCP4.5 and RCP8.5, during the expected periods, compared to the baseline period for irrigation treatments, fixed and increased $CO_2$for Sana'a

Conclusions

The results showed that full irrigation (I_1) achieved maximum grain and biomass yields during the 2023-2024 growing seasons, while deficit irrigation (I_2, I_3) led to adecrease. However, moderate deficit irrigation (I_2) achieved the highest water productivity (51 and 52 kg m^{-3}), respectively, indicating wheat's ability to withstand controlled water stress with relatively limited yield loss. This makes this strategy effective for improving irrigation efficiency under water scarcity conditions. The AquaCrop model demonstrated strong agreement between measured and simulated grain and biomass yields during the calibration and the validation periods (100, 100 and 88, 85%), respectively, confirming its reliability in assessing crop responses to irrigation and climate variability at the local level. While climate is expected indicate rising temperatures and altered rainfall patterns in the study area, which are likely to increase water stress and reduce wheat productivity if atmospheric CO_2 concentrations remain constant. Conversely, scenarios with higher CO_2 concentrations will partially mitigate these negative impacts by improving water use efficiency and reducing actual evaporation, leading to increased simulated crops. Overall, the findings highlight the importance of adaptive irrigation management for the sustainability of wheat production under future climatic conditions in the study area, and future researches should expand this approach to multiple sites, incorporate longer climate records, and employ multi-model analyses to reduce uncertainty and improve the accuracy of climate impact assessments.

Acknowledgments

We extend my sincere gratitude and deep respect, and gratitude to everyone who lent a helping hand and provided support in completing this research, from the initial planning stages to its final publication. It includes individuals, groups.

Conflict of interest

We acknowledge and declare that there are no conflicts of interest or personal relationships that could influence the work in this research, nor does it conflict with the interests of others.

Funding Declaration

No funding was allocated for this article.

Author Contribution

The first author wrote the original draft, edited it, and finalized it with the other authors. All authors read the draft and agreed to submit it to the journal.

References

Aghajanloo, M. B., and Nikbakht, J. (2023). Simulated and observed effects of the AquaCrop model in deficit irrigation management of winter wheat in the Iranian region. *Water and Soil Science, 33*(2), 23-34. file:///C:/Users/user/Downloads/Documents/458-282633-x-1163334.pdf

Ainsworth, E. A., and Long, S. P. (2005). What have we learned from 15 years of free-air CO2 enrichment (FACE)? A meta-analytic review of the responses of photosynthesis, canopy properties, and plant production to rising CO2. *New Phytologist*, 165(2), 351–372. https://doi.org/10.1111/j.1469-8137.2004.01224.x

Akol, A. M., Hassan, D. F., Mohammed, R. J., Al Janaby, Z. A. A., Kadium Abed, M. A., Hussain, S., Nassif, N., Jaddoa, K. A., and Razzaq, H. K. (2024). Optimizing wheat yield and water use efficiency using the AquaCrop model calibration and validation in various irrigation and tillage systems under climate change. *Soil Science Annual*, 75(3). 1-12. https://doi.org/10.37501/soilsa/195823

Al-Dobaee, H. Sh. (2016). *Assessing the influence of climate change on cereal crop production in Dhamar*. Master's Thesis, Water and Environment Center, Sana'a University.

Al-Durai, R. Z., Janad, A. K., and Nimr, Y. M. (2025). Evaluation of the AquaCrop mathematical model for deficit irrigation management of sorghum. *Damascus University Journal of Agricultural Sciences, 40*(2), 317-330.

Al-Saadi, M. A. (2022). *Evaluation of the AquaCrop mathematical model for deficit irrigation management of sorghum* (*Zea mays* L.), Master's Thesis, Faculty of Agriculture, Damascus University.

Asseng, S., Ewert, F., Martre, P., Rötter, R. P., Lobell, D. B., Cammarano, D., Kimball, B. A., Ottman, M. J., Wall, G. W., White, J. W., Reynolds, M. P., Alderman, P. D., Prasad, P. V. V., Aggarwal, P. K., Anothai, J., Basso, B., Biemath, C., Challinor, A. J., De Sanctis, G., Zhu, Y. (2015). Rising temperatures reduce global wheat production. *Nature Climate Change*, *5*(2), 143–147. https://doi.org/10.1038/nclimate2470

Bouras, E., Jarlan, L., Khabba, S., Er-Raki, S., Dezetter, A., Sghir, F., and Tramblay, Y. (2019). Assessing the impact of global climate change on irrigated wheat yields and water requirements in a semi-arid environment of Morocco. *Scientific Reports*, *9*(1), 1-14. https://doi.org/10.1038/s41598-019-55251-2

Dercas, N., Dalezios, N. R., Spyropoulos, N. V., and Psomiadis, E. (2022). AquaCrop simulation of winter wheat under different N management practices. *Hydrology, 9*(4), 1-20. https://doi.org/10.3390/hydrology9040056

ESCWA. (2019). *Assessing The Impact of Changes in Available Water on Crop Productivity*: Case Study Report in Yemen, Palestine, Iraq, Lebanon, Jordan, Morocco, Tunisia, Egypt, and Sudan. United Nations Economic and Social Commission for Western Asia.

ESCWA, ACSAD, and GIZ. (2017). *Integrated vulnerability assessment: Arab Regional Applications (RICCAR Technical Note)*. United Nations Economic and Social Commission for Western Asia (ESCWA).

Halawa, B. B. (2022). *Assessing the impact of climate change on sorghum productivity using the AquaCrop program at the Al-Mukhtariyeh Research Station in Homs Governorate*. Master's Thesis, Al-Baath University, Faculty of Civil Engineering.

Hassan, D., Ati, A., and Naima, A. (2023). Evaluation of the performance of the AquaCrop model under different irrigation and cultivation methods and their effect on water consumption. *Iraqi Journal of Agricultural Sciences*, *54*(2), 478–490. https://doi.org/10.36103/ijas.v54i2.1724

Kale, S., and Madenoğlu, S. (2018). Evaluating the AquaCrop model for winter wheat under various irrigation conditions in Turkey. *Journal of Agricultural Sciences*, *24*(2), 205–217. https://doi.org/10.15832/ankutbd.446438

Ministry of Agriculture, Fisheries and Water Resources. (2024). *Annual Agricultural Statistics Book* for the Year 2024, Yemen.

Nematallah, Y. O., and Kasem, A. A. (2021). Assessment of the AquaCrop model in simulating wheat crop water use and productivity in Middle Egypt. *Middle East Journal of Applied Sciences, 11*(3), 500–510. https://silice.csic.es/publication/2153df66-01c0-432c-9574-f14707f2d538

Raes, D., Steduto, P., Hsiao, T. C., and Fereres, E. (2023). *Reference manual of AquaCrop Version 7.1 Annexes*. Food and Agriculture Organization of the United Nations.

Saif, A. A., Al-Ashwal, H. H., and Al-Kharasani, A. A. (2020). Climate change and its impact on the productivity of some economic crops in the Republic of Yemen. *Syrian Journal of Agricultural Research*, 3(7), 246–258. https://agri-research-journal.net/SjarEn/?p=2550

Steduto, P., Hsiao, T. C., Raes, D., and Fereres, E. (2012). *Crop yield response to water* (FAO Irrigation and Drainage Paper No. 66). Food and Agriculture Organization of the United Nations.

Tirfi, A. G., and Oyekale, A. S. (2022). Impact of climate change on yields of wheat in Ethiopia: An augmented Cobb-Douglas production function approach. *Journal of Agricultural, Food and Environmental Sciences*, *76*(1), 34–47. https://doi.org/10.55302/JAFES22761034t

Willmott, C. J., Robeson, S. M., and Matsuura, K. (2013). A refined index of model performance. *International Journal of Climatology*, *33*(4), 1053–1056. https://doi.org/10.1002/joc.2419